文章编号:1001 - 9014(2011)06 - 0486 - 05

Microwave-modulated reflectance spectroscopy in the GaAs/AlGaAs heterostructure

QIAN Xuan, GU Xiao-Fang, JI Yang*

(State Key Laboratory of Superlattice and Microstructures, Institute of Semiconductors, Chinese Academy of Sciences, Beijing 100083, China)

Abstract: A microwave-modulated reflectance spectroscopy (MMRS) measurement system was constructed. This MMRS technique was used to identify a transition from holes in valence band to electrons in the ground subband (GS) of the two-dimensional electron system (2DES) formed in a GaAs/AlGaAs heterostructure sample. The temperature (T) dependence of the MMRS shows a blue shift of the energy gap with increasing T, while the magnetic field (B) dependence of the MMRS shows a red shift of the energy gap with increasing B. Both phenomena are attributed to the band-filling effect of holes in valence band in the GaAs/AlGaAs heterostructure. A theoretical simulation based on Kramers-Kronig relation was also presented which was similar with the experimental data.

Key words: microwave-modulated reflectance spectroscopy; two-dimensional electron system

PACS: 78.40.Fy, 78.67.De

GaAs/AlGaAs 异质结的微波调制反射谱

钱 轩, 谷晓芳, 姬 扬*

(中国科学院半导体研究所 超晶格国家重点实验室, 北京 100083)

摘要: 基于搭建的微波调制反射谱测量系统(MMRS), 确定了GaAs/AlGaAs异质结构中价带空穴到二维电子系统(2DES)电子基态(GS)的跃迁. 微波调制反射谱与温度的依赖关系表明, 随着测量温度的升高, 能带带隙发生了蓝移现象; 而其与磁场的依赖关系表明, 随着测量磁场的增大, 能带带隙则发生了红移现象; 它们均与GaAs/AlGaAs异质结构中价带空穴的带填充效应有关. 基于Kramers-Kronig关系的理论模拟给出了和实验测量相似的结果.

关 键 词: 微波调制反射谱; 二维电子系统

中图分类号: O472+.3; O482.55; O514.2 **文献标识码**: A

Introduction

Observing the slight difference in the light reflectance spectrum induced by a perturbation, for example, laser, electric field, or magnetic field, to semiconductor materials, one may obtain much information about the samples under study and gain insight about the related physical processes. A number of modulation spectroscopies have been developed[1-4], among which the electroreflectance (ER) method and the photoreflectance (PR) method are most widely used. Despite the obvious advantages of such techniques, for example, wide temperature range and non-contact measurement, some drawbacks impede their applicability. The ER method needs special sample preparations while the PR method may have problems in separating the PR and photoluminescence (PL) spectra at low temperature[5], which happens due to the huge increase (by several orders of magnitude) of the PL amplitude which affects PR measurements.

Received date: 2010 - 12 - 27, **revised date**: 2011 - 06 - 14 **收稿日期**: 2010 - 12 - 27, **修回日期**: 2011 - 06 - 14

Foundation items: National Nature Science Foundation(10674129); National Basic Research Program(2009CB929301)

Biography: QIAN Xuan(1984-), Male, Jinhua China, Ph. D. Research field is semiconductor spintronics and microwave - modulated reflectance spectroscopy. E-mail: qianxuan@semi.ac.cn.

* **Corresponding Author**: E-mail: jiyang@red.semi.ac.cn.

A method based on modulation of the reflection of the probe light by microwave, a microwave-modulated reflectance spectroscopy (MMRS), may preserve the advantages of both PR and ER methods[4]. In this case, such a modulation is provided by a microwave, whose electric field accelerates the free carriers but it is insufficient for the production of new nonequilibrium carriers. The net effect of such acceleration increases the mean kinetic energy of the free carriers (a heating effect) and changes the optical absorption near the bandgap, thus leading to a change of the reflectance.

Here we report the experimental realization of MMRS measurement system which can be used in liquid helium temperature and rather high magnetic field. Using this system, we observed a transition from holes in valence band to electrons in the ground state (GS) of a two-dimensional electron system (2DES) embedded in a GaAs/AlGaAs heterostructure. The temperature dependence of the MMRS shows a blue shift of the energy gap with increasing temperature, while the magnetic field dependence of the MMRS shows a red shift of the energy gap with increasing magnetic field, which agrees with our theoretical simulation qualitatively.

1 Experimental details

Fig. 1 shows a schematic view of the MMRS measurement system. It has a light source of a mode-locked Ti: sapphire pulse laser (Coherent 900D), which has a temporal duration of 150 fs and a repetition rate of 76 MHz, with its wavelength being tunable from 790 nm to 840 nm continuously by a stepper motor (Zolix SC300). A half-reflected mirror splits the laser beam for balanced detection and a 25 cm-focal length-lens focuses the laser beam to a spot of ~100 μm in diameter on the sample, which is mounted on a magneto-optical cryostat (Oxford Instruments) with a superconducting split-coil magnetic field up to 10 T and a tunable temperature range from 1.5 K to 300 K. A customer-designed sample rod with two rectangular wave guides for 8 mm microwave is utilized to radiate the Ka-band microwave (with frequency ranging from 26 GHz to 40 GHz) onto the sample. A microwave generator with a tunable frequency of 33.5 ~ 36.5 GHz and a maximal power output of 50 mW is used. The microwave power available on the sample is about 5 mW and modulated at a frequency of 173 Hz, with its alternating electric field parallel or perpendicular to the sample surface[6]. The reflected light from the sample is collected with a photoreceiver (New focus 2307), which is balanced by a laser beam that is split by the half-reflected mirror. The MMRS signal is measured with lock-in technique at the modulation frequency 173 Hz. The stepper motor, microwave generator, magneto-optical cryostat, and the lock-in amplifier (Stanford Research Systems SR830) are all controlled by a personal computer with relay control boards (Serial Card and GPIB Card) and LABVIEW software.

Our sample was grown by molecular beam epitaxy (MBE). The growth sequence of the layer structures was as follows: a buffer layer of 20 periods of 10 nm GaAs/AlAs superlattice was first grown on a semi-insulating (100) GaAs, followed by a 60-nm-thick intrinsic GaAs layer. On the top of it was a $Al_xGa_{1-x}As$ layer, which consisted of a 10-nm-thick $Al_{0.3}Ga_{0.7}As$ layer and a 50-nm-thick $Al_xGa_{1-x}As$ layer with x varying linearly from 0.3 to 0.1 in the growth direction. The structure was completed with a 65 nm $Al_{0.1}Ga_{0.9}As$ layer and a 20 nm GaAs cap layer. The 65-nm-thick $Al_{0.1}Ga_{0.9}As$ layer was δ doped with $2 \times 10^{11}\,cm^{-2}$ Si dopant.

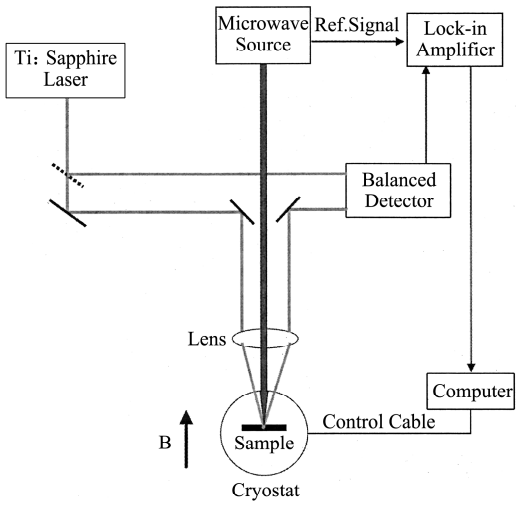

Fig. 1　Schematic diagram of the microwave-modulated reflectance spectroscopy measurement system
图 1　微波调制反射谱测量系统的示意图

2 Results and discussion

Fig. 2 shows the MMRS curves of the GaAs/AlGaAs heterostructure sample measured with the electric field of microwave parallel and perpendicular to the sample surface, respectively. Both traces have peaks at the same positions but their magnitude is different from each other, which may be caused by the different transmission loss of microwave along the two orthogonal waveguides in the sample rod. The MMRS were also measured at different microwave modulation frequency (33.5GHz and 36GHz) and their signals have same peak positions as well. The same position of peaks means that the MMRS signal is independent of either the irradiation direction or the frequency of microwave, therefore this is irrelevant to microwave resonance phenomenon. The microwave just plays the role of heating. Because of the heating effect induced by the microwave, the Fermi-Dirac distribution of electrons in conduction band and holes in valence band would change, so does the optical absorption near the bandgap, $\Delta\alpha$, which can be expressed as:

$$\Delta\alpha(E,T) = A[f_v(E,T+\Delta T)(1-f_c(E,T+\Delta T)) - f_v(E,T)(1-f_c(E,T))] \quad , \quad (1)$$

where A is a constant, ΔT is a temperature increase induced by the heating effect of the microwave, f_v and f_c are the Fermi-Dirac distribution of electrons in valence band and conduction band, respectively. The change of absorption coefficient, $\Delta\alpha$, and the change of refractive index, Δn, are related to each other by the famous Kramers-Kronig relation[7]

$$\Delta n(E) = \frac{2c\hbar}{e^2} P\int_0^\infty \frac{\Delta\alpha(E',T)}{E'^2 - E^2} dE' \quad , \quad (2)$$

where c is the speed of light, e is the electron charge, E is the photo energy, and P indicates the principal value of the integral. For further simplification, we ignore all the constants in the above equations, neglect the change of f_v, since the Fermi energy is much higher than the maximum of the valence band, and assume that the change of reflectance is proportional to the change of refractive index. With such simplifications and combining equations (1) and (2):

$$\frac{\Delta R}{R} \propto \int_0^\infty \frac{f_c(E',T+\Delta T) - f_c(E',T)}{E'^2 - E^2} dE' \quad . \quad (3)$$

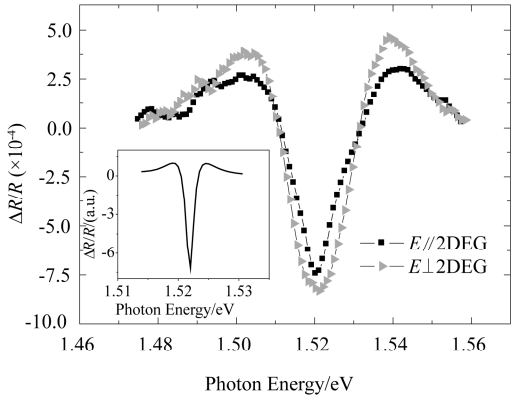

Fig. 2 The MMRS curves of the GaAs/AlGaAs heterostructure sample measured with the electric field of microwave parallel and perpendicular to the sample surface, respectively. Inset is $\Delta R/R$ calculated with Eq. 3

图2 微波电场平行和垂直于样品表面时的 GaAs/AlGaAs 异质结 MMRS 曲线. 插图是根据公式(3)计算得到的 $\Delta R/R$

The values of $\Delta R/R$ can be calculated by numerical integration, as shown in the inset in Fig. 2 (with typical values of $\Delta R/R$ estimated to be about 10^{-4} for E = 1.525eV and T = 20K). The calculated curve of $\Delta R/R$ agrees well with the experimental data except that its spectral width is a bit smaller than the experimental observation which may be caused by the spectral broadening of the pulse laser and some more complicated mechanisms. In the following discussion, we focus on the change of peak positions and have not taken the change of spectral width into account.

Fig. 3 shows the MMRS curves of the GaAs/AlGaAs heterostructure at several different temperatures with the microwave electric field being perpendicular to the sample surface. As the temperature increases, the amplitude of the MMRS signal drops rapidly. The reason is that ΔT induced by the microwave heating does not vary much while ambient temperature rises, lead to a decreasing $\Delta T/T$, in other words, the microwave's heating effect becomes weaker. A blue shift of the curves from 1.521eV to 1.527eV takes place while temperature goes from 3K up to 40K. Both the Fermi energy of conduction band and the bandgap of GaAs/AlGaAs material depend on temperature[8]. The former leads to a blue shift but it is too small(~0.1 meV) at such a low temperature to explain the experimental data, while the latter mechanism leads to a small red shift. We attribute this blue shift to the excitation of e-

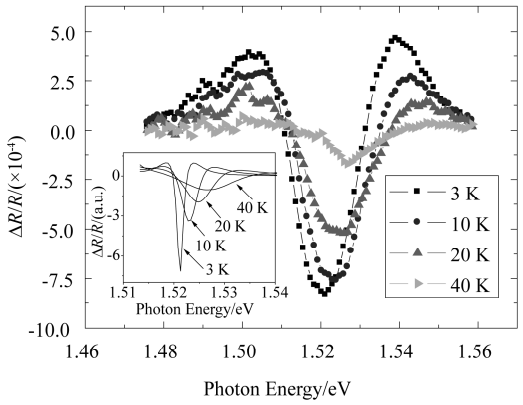

Fig. 3　The MMRS curves of the GaAs/AlGaAs heterostructure at different temperatures with electric field of microwave perpendicular to the sample surface. Inset: $\Delta R/R$ calculated with Eq. 3, with the band-filling effect taken into account.

图 3　微波电场垂直于样品表面,不同温度下的 GaAs/AlGaAs 异质结 MMRS 曲线. 插图为根据公式(3)得到的 $\Delta R/R$

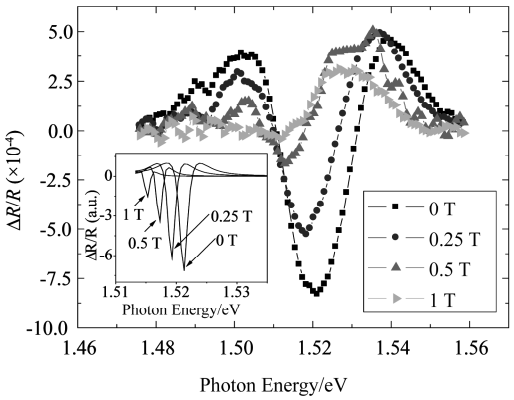

Fig. 4　The MMRS curves of the GaAs/AlGaAs heterostructure with different magnetic fields perpendicular to the sample surface at 3K. Inset: $\Delta R/R$ calculated with Eq. 3, with the band-filling effect taken into account

图 4　垂直于样品表面的不同磁场下,3K 时 GaAs/AlGaAs 异质结 MMRS 曲线. 插图为根据公式(3)得到的 $\Delta R/R$

lectrons in the valence band into the impurity band of the GaAs/AlGaAs heterostructure as temperature goes up, thus leading to much more holes in the valence band. Due to this band-filling effect in the valence band[9], a blue shift of the transition energy between holes and electrons in the GS takes place as temperature increases. The band-filling effect was estimated according to the Nilsson approximation at $T = 20$ K[10]: the change of 6 meV in Fermi level in the valence band corresponds to impurity band concentrations of about $10^{12}\,\mathrm{cm}^{-2}$, which is reasonable in our sample grown by MBE. The inset of Fig. 3 shows simulated curves of $\Delta R/R$ as calculated from Eq. 3, with the band-filling effect taken into account.

Fig. 4 shows the MMRS measured at 3K of the GaAs/AlGaAs heterostructure with different magnetic fields perpendicular to the sample surface. As the magnetic field increases, microwave-induced heating effect may be reduced as a result of even stricter selection rules, therefore, ΔT and $\Delta T/T$ decrease and the amplitude of MMRS signal drops as well. A red shift from 1.521eV to 1.511eV occurs while magnetic field changes from zero to 1T. The magnetic field weakens the microwave-induced heating effect, therefore it reduces the band-filling effect of holes in valence band and causes a red shift of the MMRS' dip. The inset of Fig. 4 shows a simulating result for such a process.

3　Conclusions

In summary, we constructed a MMRS measurement system and demonstrated its performance in a GaAs/AlGaAs heterostructure. The MMRS signal does not depend on the irradiation direction of microwave, suggesting that the main effect of the microwave here is to heat the electrons in the 2DES. Also a blue shift of the energy gap with increasing temperature and a red shift of the energy gap with increasing magnetic are observed, which are related to the band-filling effect of holes in valence band in the GaAs/AlGaAs heterostructure. We give a theoretical simulation based on Kramers-Kronig relation which agrees with our experimental data qualitatively. The apparatus works well and the MMRS would be a helpful tool in the study of materials' energy band structures.

4　Acknowledgements

We thank Professor NIU Zhi-Chuan for providing high quality sample. This work was supported by the NSFC under Grant No. 10911130232 under Contract No. 10674129 and the National Basic Research Program of China under Grant No. 2009CB929301.

REFERENCES

[1] Nahory R E, Shay J L. Reflectance modulation by the surface field in GaAs[J]. *Phys. Rev. Lett.*, 1968, **21**(23): 1569 – 1571.

(下转 510 页)

响ZnS薄膜的晶体结构和表面形貌. 退火前后的ZnS薄膜都具有均匀、致密的表面结构,且晶粒大小维持在29 nm左右不变. 然而,退火显著影响ZnS薄膜的发光性能. 低温退火时,PL谱表现出多个发光峰,而当退火温度升至500℃时, PL谱则表现为单一发光峰. 退火对ZnS薄膜发光性能的影响是通过影响薄膜中缺陷态的种类和浓度来实现的.

REFERENCES

[1] Asenjoa B, Chaparroa A M, Gutierrez M T, *et al.* Study of $CuInS_2$/ZnS/ZnO solar cells with chemically deposited ZnS buffer layers from acidic solutions[J]. *Sol. Energy Mater. Sol. Cells*,2008,**92**(3):302 - 306.

[2] Deulkara S H, Bhosalea C H, Sharonb M. A comparative study of structural, compositional, thermal and optical properties of non stoichiometric (Zn,Fe)S chalcogenide pellets and thin films[J]. *J. Phys. Chem. Solids*,2004,**65**(11):1879 - 1885.

[3] Sartale S D, Sankapal B R, Lux-Steiner M, *et al.* Preparation of nanocrystalline ZnS by a new chemical bath deposition route[J]. *Thin Solid Films*, 2005, **480 - 481**: 168 - 172.

[4] Durrani S M, Al-Shukri A M, Iob A, *et al.* Optical constants of zinc sulfide films determined from transmittance measurements[J]. *Thin Solid Films*,2000,**379**(1-2):199 - 202.

[5] Ghosh P K, Jana S, Nandy S, *et al.* Size-dependent optical and dielectric properties of nanocrystalline ZnS thin films synthesized via rf-magnetron sputtering technique[J]. *Mater. Res. Bull.*,2007,**42**(3):505 - 514.

[6] Yazici A N, Oztas M, Bedir M. Effect of sample producing conditions on the thermoluminescence properties of ZnS thin films developed by spray pyrolysis method[J]. *J. Lumi.*, 2003,**104**(1-2):115 - 122.

[7] Hillie T K, Current C, Swart H C. ZnS thin films grown on Si (100) by XeCl pulsed laser ablation[J]. *Appl. Surf. Sci.*,2001,**177**(1-2):73 - 77.

[8] Roy P, Ota J R, Srivastava S K. Crystalline ZnS thin films by chemical bath deposition method and its characterization [J]. *Thin Solid Films*,2006,**515**(4):1912 - 1917.

[9] Ates A, Yıldırım M A, Kundakcı M, *et al.* Annealing and light effect on optical and electrical properties of ZnS thin films grown with the SILAR method[J]. *Mater. Sci. Semicond. Process.*,2007,**10**(6):281 - 286.

[10] Cullity B D. *Elements of X-ray Diffraction*[M]. Reading: Addison-Wesley,1978,284.

[11] Mastio E A, Craven M R, Cranton W M, *et al.* The effects of KrF pulsed laser and thermal annealing on the crystallinity and surface morphology of radiofrequency magnetron sputtered ZnS:Mn thin films deposited on Si[J]. *J. Appl. Phys.*, 1999,**86**(5):2562 - 2570.

[12] Lu H Y, Chu S Y, Tan S S. The characteristics of low-temperature-synthesized ZnS and ZnO nanoparticles[J]. *J. Cryst. Growth*,2004,**269**(2-4):385 - 391.

[13] Lee J C, Park D H. Self-defects properties of ZnS with sintering temperature[J]. *Mater. Lett.*, 2003, **57**(19): 2872 - 2878.

[14] Denzler D, Olschewski M, Sattler K. Luminescence studies of localized gap states in colloidal ZnS nanocrystals [J]. *J. Appl. Phys.*,1998,**84**(5):2841 - 2845.

[15] Kurbatov D, Kosyak V, Opanasyuk A, *et al.* Native point defects in ZnS films[J]. *Physica B*,2009,**404**(23-24): 5002 - 5005.

[16] Chen W, Wang Z G, Lin Z J, *et al.* Absorption and luminescence of the surface states in ZnS nanoparticles[J]. *J. Appl. Phys.*,1997,**82**(6):3111 - 3115.

[17] Motlan, Zhu G H, Drozdowicz-Tomsia K, *et al.* Annealing of ZnS nanocrystals grown by colloidal synthesis[J]. *Opt. Mater.*,2007,**29**(12):1579 - 1583.

(上接489页)

[2] DOU Hong-Fei, LU Wei, CHEN Xiao-Shuang, *et al.* Thermo-modulation reflectance spectra assisted by the space thermal gradient[J]. *J. Infrared Millim. Waves*(窦红飞,陆卫,陈效双,等. 空间热梯度辅助的热调制反射光谱. **红外与毫米波学报**),1999,**18**(1):93 - 96.

[3] Mendez E E, Chang L L, Landgren G, *et al.* Observation of superlattice effects on the electronic bands of multilayer heterostructures[J]. *Phys. Rev. Lett.*,1981,**46**(18):1230 - 1234.

[4] Chernikov M A, Ryabushkin O A. Microwave modulated light reflection in semiconductors [J]. *Technical Physics Letters*,2001,**27**(12):1038 - 1040.

[5] Glembocki O J, Shanabrook B V, *Photoreflectance spectroscopy of microstructures, in semiconductors and semimetals* [M] Academic Press, New York,1992:221 - 292.

[6] Luo H H, Qian X, Gu X F, *et al.* Effect of Ka-band microwave on the spin dynamics of electrons in a GaAs/$Al_{0.35}Ga_{0.65}As$ heterostructure[J]. *Appl. Phys. Lett.*,2009,**94**(19):192107.

[7] Stern F. Dispersion of the index of refraction near the absorption edge of semiconductors[J]. *Phys. Rev. A*,1964, **133**(6A):1653 - 1664.

[8] Varshni Y P. Temperature dependence of the energy gap in semiconductors[J]. *Physica*,1967,**34**:149 - 154.

[9] Bennett B R, Soref R A, Del Alamo J A. Carrier-induced change in refractive index of InP, GaAs, and InGaAsP[J]. *IEEE J. Quantum Electron.*,1990,**26**(1):113 - 122.

[10] Nilsson N G, Empirical approximations for the Fermi energy in a semiconductor with parabolic bands[J]. *Appl. Phys. Lett.*,1978,**33**(7):653 - 654.